Protist, Vol. 158, 209—227, April 2007
http://www.elsevier.de/protis
Available online 24 January 2007

Protist

ORIGINAL PAPER

Morphology and Phylogeny of the Pseudocolonial Dinoflagellates *Polykrikos lebourae* and *Polykrikos herdmanae* n. sp.

Mona Hoppenrath[1], and Brian S. Leander

Canadian Institute for Advanced Research, Program in Evolutionary Biology, Departments of Botany and Zoology, University of British Columbia, Vancouver, BC, V6T 1Z4 Canada

Submitted September 9, 2006; Accepted December 1, 2006
Monitoring Editor: Michael Melkonian

Both the photosynthetic and heterotrophic forms of the only known marine benthic (sand-dwelling) species of *Polykrikos*, namely *P. lebourae*, were investigated using light and electron microscopy and molecular phylogenetic analyses. The pseudocolonies usually contained eight integrated zooids and two nuclei. Pseudocolonies consisting of four or five zooids and one nucleus were observed for the first time for this species; some of these reduced pseudocolonies contained plastids, while others were heterotrophic and contained taeniocyst—nematocyst complexes. The ultrastructure of the plastids in *P. lebourae* did not conform to the organization of thylakoids and enveloping membranes present in the peridinin-containing plastids of other photosynthetic dinoflagellates (i.e. stacks of 3 thylakoids and 3 outer membranes). Instead, the plastids in *P. lebourae* had thylakoids arranged in pairs and appeared to be enveloped by only two membranes. Molecular phylogenetic data using small subunit rDNA demonstrated that the photosynthetic and heterotrophic forms of *P. lebourae* represent two distinct clades. The more inclusive clade containing both forms of *P. lebourae* was most closely related to heterotrophic polykrikoids, namely *P. kofoidii*. These results led us to conclude that the photosynthetic and heterotrophic forms of *P. lebourae* are in fact two distinct lineages, and the heterotrophic form is described here as *Polykrikos herdmanae* n. sp.

Key words: dinoflagellate; Dinophyceae; *Gymnodinium*; plastid; *Polykrikos*; *P. lebourae*; *P. herdmanae*; phylogenetic analysis; SSU rDNA; ultrastructure.

Introduction

The most distinctive feature of the athecate dinoflagellate genus *Polykrikos* Bütschli is the formation of multinucleated 'pseudocolonies' comprised of an even number of zooids that are otherwise similar in morphology to individual dinoflagellates in external view. The zooid sulci are fused together, but every zooid has its own cingulum and pair of flagella. A pseudocolony often has half the number of nuclei than it has zooids. Trichocysts, nematocysts, taeniocysts, mucocysts, and plastids have all been reported from different members within the group. The genus currently comprises four species: *P. schwartzii* Bütschli — the type species, *P. kofoidii* Chatton, *P. lebourae* Herdman, and *P. grassei* Lecal. The morphological features,

[1]Corresponding author;
fax +1 604 822 6089
e-mail hoppen@interchange.ubc.ca (M. Hoppenrath).

doi:10.1016/j.protis.2006.12.001

systematic history, and taxonomic issues within the polykrikoid dinoflagellate species is summarized elsewhere (Hoppenrath and Leander 2007). All known polykrikoid species are marine and planktonic, except *P. lebourae*, which inhabits sandy interstitial environments.

Polykrikos lebourae has pseudocolonies consisting of eight zooids and two nuclei and lacks visible borders between zooids (Balech 1956; Dragesco 1965; Herdman 1923; Hoppenrath 2000; Fig. 1A—D). Moreover, although a heterotrophic form has been described and is included in the original species description, *P. lebourae* was in most cases described as photosynthetic (Balech 1956; Dragesco 1965; Herdman 1923; Hoppenrath 2000). A potential to disassemble into smaller zooid stages with only one nucleus, as described for *P. kofoidii* and *P. schwartzii* (e.g., Nagai et al. 2002), has not been recorded for *P. lebourae*. The heterotrophic form of *P. lebourae* (almost) always contains complex extrusomes or 'taeniocyst—nematocyst complexes', which have been occasionally observed in photosynthetic forms as well (Dragesco 1965; Hoppenrath 2000). It is unclear whether the photosynthetic and heterotrophic forms of *P. lebourae* constitute two separate lineages or represent variability within one species.

Molecular phylogenetic data have demonstrated that the photosynthetic form of *P. lebourae* is most closely related to heterotrophic polykrikoids, namely *P. kofoidii*, and more distantly related to phototrophic polykrikoid species, such as *Pheopolykrikos hartmannii* (Zimmermann) Matsuoka and Fukuyo, originally described as *Polykrikos hartmannii* Zimmermann (Hoppenrath and Leander 2007). Because there are no ultrastructural data available for *P. hartmannii*, it is difficult to evaluate the plastid morphotype and to infer the history of photosynthesis in the polykrikoid lineage. Therefore, it is currently unclear whether photosynthesis in *P. lebourae* was retained from a distant photosynthetic ancestor with the usual peridinin-containing dinoflagellate plastid or perhaps was regained via an independent tertiary or serial secondary endosymbiosis. Three possible scenarios can explain photosynthesis in *P. lebourae*: (1) *P. lebourae* has typical peridinin-containing plastids, like *Gymnodinium fuscum* (Ehrenberg) Stein, and the heterotrophic form subsequently lost photosynthesis and represents a different species; (2) *P. lebourae* is ancestrally heterotrophic and the photosynthetic form subsequently acquired plastids via an endosymbiotic event; (3) *P. lebourae* is ancestrally heterotrophic and able to temporary retain plastids (and photosynthesis) via kleptoplastidy.

An obvious and necessary step toward addressing these scenarios is to generate ultrastructural data from the phototrophic form of *P. lebourae*. Some ultrastructural data are already available for three heterotrophic relatives: *Polykrikos kofoidii* (Bradbury et al. 1983; Westfall et al. 1983), *P. grassei* (Lecal 1972) and *P. schwartzii* (e.g., Chatton 1914; Chatton and Grassé 1929; Greuet 1972; Greuet and Hovasse 1977). However, there are significant doubts about the validity of *P. grassei*, because this species has only been recorded once and has pseudocolonies that are extremely similar to *P. kofoidii* (Greuet and Hovasse 1977; Hoppenrath and Leander 2007; Lecal 1972; Sournia 1986). Nonetheless, our aims in this paper are to demonstrate (1) the ultrastructural organization of the *P. lebourae* cell, especially the plastid, in order to better understand character evolution within the group, and (2) the phylogenetic distance between the heterotrophic and photosynthetic forms

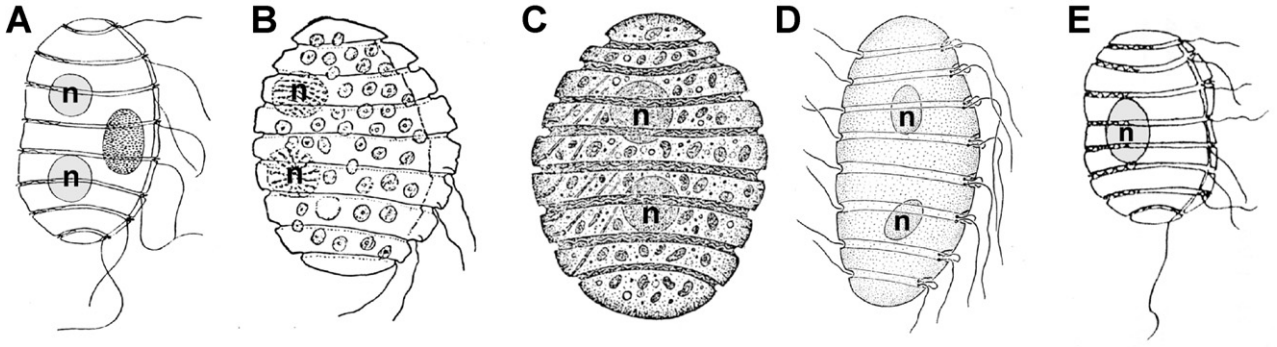

Figure 1. Reproduced line drawings from *Polykrikos lebourae*. **A**. Redrawn from Herdman 1923. **B**. Redrawn from Balech 1956. **C**, **D**. Redrawn from Dragesco 1965. **E**. Redrawn from Herdman 1921. n = nucleus.

of *P. lebourae* using a molecular phylogenetic approach.

Results

Morphology of the Photosynthetic Form of *Polykrikos lebourae*

Pseudocolonies of the photosynthetic form of *P. lebourae* (from Canadian and German sites) generally consisted of eight zooids and two nuclei (Fig. 2 A—E). In Canada, reduced photosynthetic pseudocolonies consisting of four zooids and one nucleus were also observed (Fig. 2 F, 2 G). Specimens with eight zooids lacked visible borders between zooids and were 50.0—90.0 μm long and 35.0—50.0 μm wide in Canada, and 37.5—75.0 μm long and 20.0—50.0 μm wide in Germany (Figs 2 A, 3 A, 3 B). The pseudocolonies were ovate in shape with the terminal zooids being about half as wide as the central zooids (Fig. 2 A—E). The acrobase (apical groove) was loop-shaped (Figs 2 B, 3 C). The pseudocolonies were obliquely flattened, and fused ventral sulci were positioned laterally on the right-hand side of the pseudocolony (Figs 2 C—E, 3 A). The fused sulcus was oriented along the longitudinal axis of the pseudocolony, was slightly curved (Fig. 3 A), and reached the antapex (Fig. 3 E). The cinguli were descending and displaced about one to two cingular widths, where the largest displacement occurred in the most anterior zooid (Fig. 3 A, 3 E). The left hand margin of the fused sulcus formed transverse bulges below the second and third cingulum, relative to the apical pole (Fig. 3 A, 3 E). Eight sets of longitudinal and transverse flagella were present (Figs 2 A, 3 A, 3 B, 3 E, 3 F). The transverse flagella did not encircle the cell completely. The two nuclei were nearly spherical and were distributed in the center of the anterior and posterior halves of the pseudocolony, respectively (Fig. 2 B, 2 C).

The photosynthetic form of *P. lebourae* possessed several small, golden-brown plastids that were spherical or spindle-shaped and contained a pyrenoid (Fig. 2 B—C). Occasionally, the plastids were concentrated around the nuclei giving the periphery of the pseudocolony a colorless appearance (Fig. 2 J). Photosynthetic specimens also contained red colored food bodies of variable number and size that were positioned in different areas of the pseudocolony (Fig. 2 D). Complex extrusomes were observed only occasionally in the photosynthetic form of *P. lebourae*. When they were visible, thin lanceolate extrusomes could be observed near the flagellar insertion zones (Fig. 2 D) or distributed throughout the pseudocolony (Fig. 2 E, 2 I). In one photosynthetic specimen from Germany, a taeniocyst-nematocyst complex like that found in heterotrophic species of *Polykrikos* was observed (Fig. 2 H).

The photosynthetic form of *P. lebourae* showed the general cytoplasmic organization of athecate dinoflagellates. The determination of whether or not the cytoplasm of the pseudocolonies is internally compartmentalized in some way was inconclusive; however, we did not find any evidence for internal septa in our micrographs. Nonetheless, these relatively large cells were highly vacuolated. In addition to the nuclei, the cytoplasm contained plastids, large vesicles, and lipoprotein droplets (Fig. 4 A). The alveolar vesicles subtending the plasma membrane were generally not well preserved in our TEM micrographs; however, these membranes were subtended by a robust, but thin epiplasm (Fig. 4 B, 4 C). Embedded within the epiplasm were spherical surface structures comprised of multiple concentric membranes (Fig. 4 B, 4 C). This multiple membrane structures could pierce the superficial layer of the epiplasm (Fig. 4 C). The pusule consisted of a main collecting chamber with associated spherical pusular vesicles (Fig. 4 D). Some vesicles budding from the main canal were surrounded by a double membrane (Fig. 4 D). The pusule opened to the outside of the cell in the flagella area of the sulcus (Fig. 4 E). Single rows of microtubules were located beneath the inner alveolar membrane (Fig. 4 E).

Three types of extrusomes were present in the photosynthetic form of *P. lebourae*. The taeniocyst was enveloped by a membrane and consisted of a densely stained body with conical neck and an apical head (Fig. 5 A). The taeniocyst body contained a posterior amorphous zone (Fig. 5 A). The neck consisted of concentric lamellae within the taeniocyst body in transverse section (Fig. 5 B). The cells contained many mucocysts (Fig. 5 C—F) that usually accumulated beneath the alveolar membranes (Fig. 5 C). These vermiform mucocysts were surrounded by a continuous set of membranes (4—6) and had a dense outer layer around a fibrillar inner core (Fig. 5 D—F). The dense apical ‘cap’ of the mucocysts was observed protruding through the alveolar membranes and the plasma membrane (Fig. 5 F). Trichocysts were enveloped by a single membrane and were composed of a column-like body with a lattice-like structure, a neck comprised of small regularly

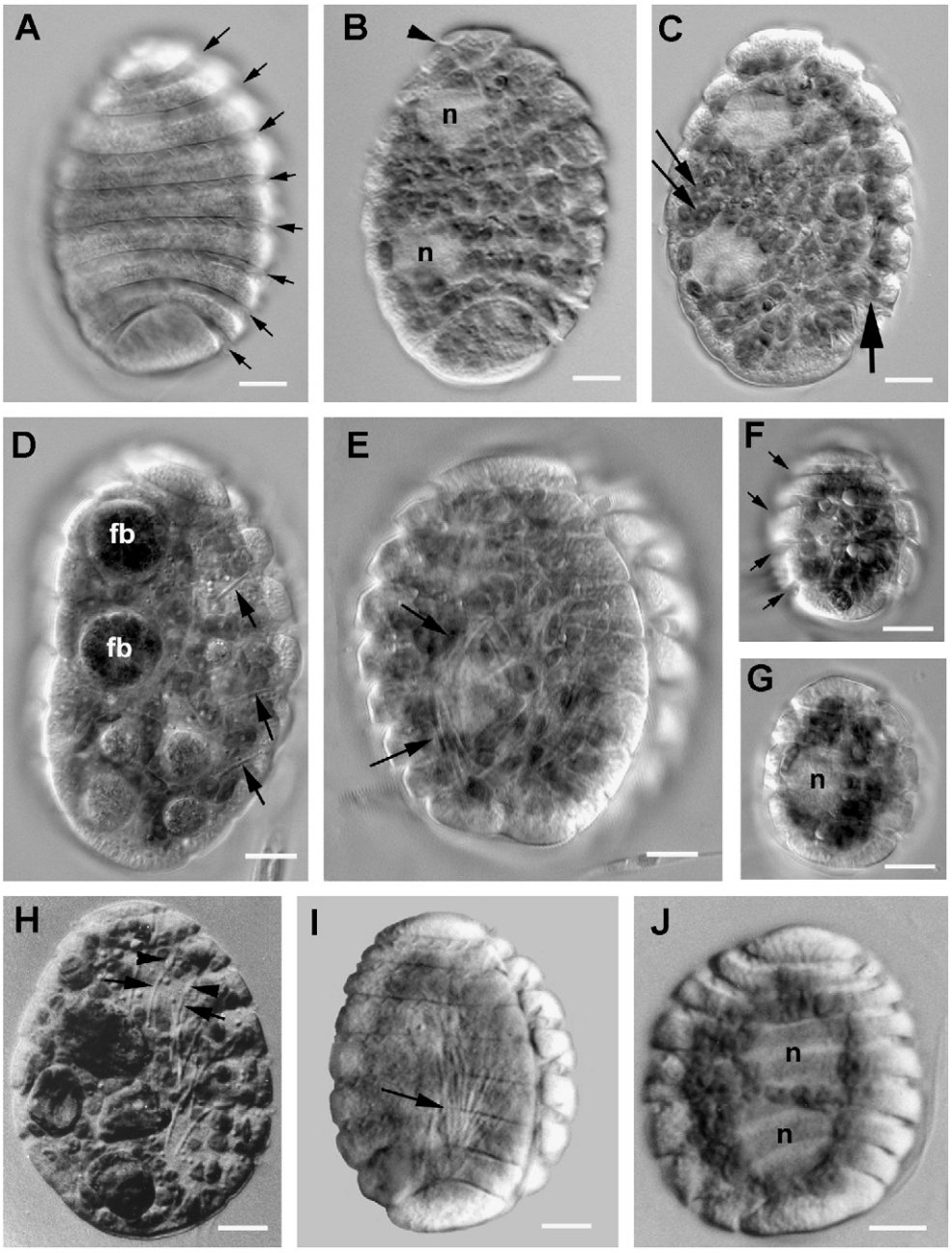

Figure 2. Light micrographs (LM) of *Polykrikos lebourae* from Canada (A—G) and Germany (H—J). **A.** Pseudocolony in focus on the eight transverse flagella within cinguli (arrows). **B.** Pseudocolony showing the relative positions of two nuclei (n) and the acrobase (arrowhead). **C.** Pseudocolony showing the abundance and distribution of plastids, each containing a single pyrenoid (arrows), and the position of the fused sulci (large arrow). **D.** Pseudocolony containing lanceolate taeniocysts positioned at the flagellar insertion areas of the sulcus (arrows) and two food bodies (fb). **E.** Pseudocolony showing the fused sucli and containing thread-like extrusomes (arrows). **F.** Pseudocolony consisting of four zooids containing plastids. Note the four cinguli (arrows). **G.** Pseudocolony consisting of four zooids containing one nucleus (n). **H.** Pseudocolony containing taeniocyst—nematocyst complexes positioned at the flagella insertion areas of the sulcus. Note the taeniocyst (arrowhead) and nematocyst (arrows) positions in the complexes. **I.** Pseudocolony showing the fused sulci and containing thread-like extrusomes (arrow). **J.** Pseudocolony with plastids concentrated around the nuclei (n), giving the pseudocolony-margin a colorless appearance. (**A—J**, Bar = 10 μm).

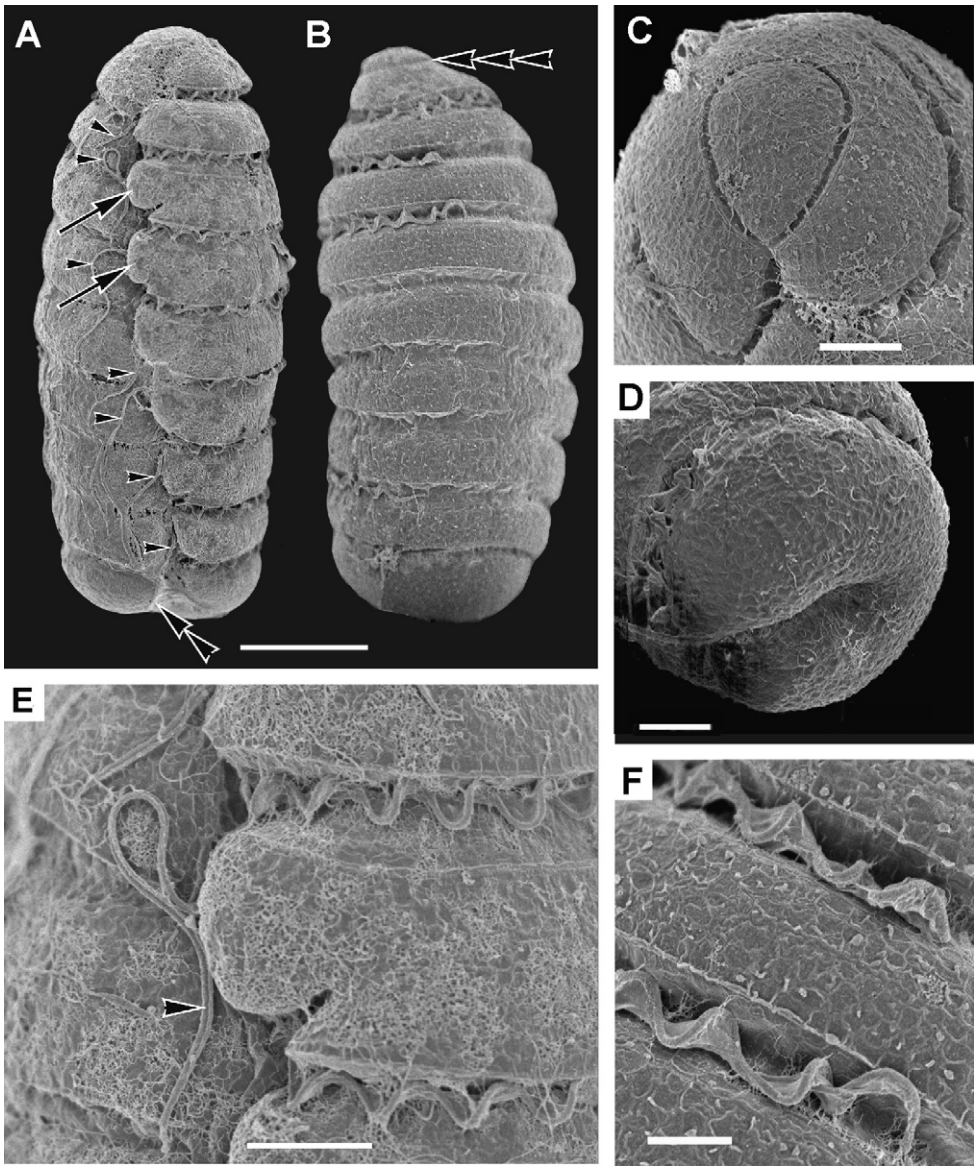

Figure 3. Scanning electron micrographs (SEM) of *Polykrikos lebourae*. **A**. SEM of the ventral side of the pseudocolony showing the fused longitudinal sulcus from which eight recurrent flagella (arrowheads) and eight coiled transverse flagella, each within a well-developed cingulum, emanate. Although the posteriormost recurrent flagellum was lost during SEM preparation, the depression within which it resides is defined by a curved ridge (double arrowheads) oriented in the transverse plane. The left hand margin of the fused sulcus formed transverse bulges (arrows) below the second and third cinguli, relative to the apical pole. **B.** SEM of the dorsal side of the pseudocolony showing eight transverse cinguli and the apical acrobase (triple arrowhead) (**A—B**, Bar = 15 μm). **C**. High magnification SEM of the apical pole showing the loop-shaped acrobase oriented in parallel with the first cingulum (Bar = 5 μm). **D**. High magnification SEM of the antapical pole showing the sulcus ending at the posterior end of the pseudocolony (Bar = 5 μm). **E**. High magnification SEM of a transverse bulge stemming from the left-hand margin of the fused sulcus showing the recurrent flagella (arrowheads) (Bar = 5 μm). **F**. High magnification SEM showing the coiled transverse flagella within cinguli and the pattern of small polygonal alveolar sacs beneath the plasma membrane (Bar = 2.5 μm).

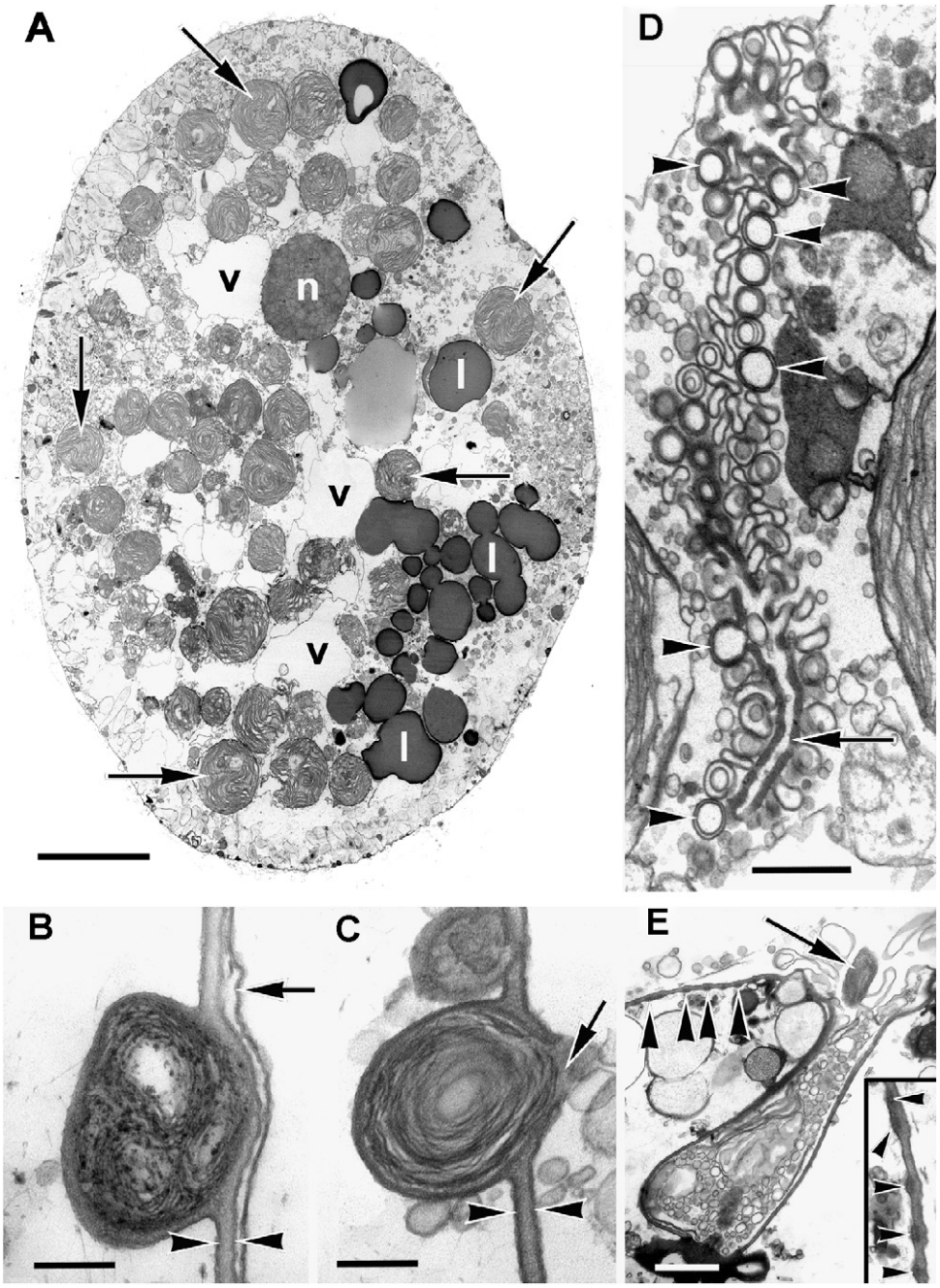

Figure 4. Transmission electron micrographs (TEM) of *Polykrikos lebourae*. **A**. Low magnification TEM showing the general organization of the cytoplasm. This oblique section contains one nucleus (n), large vesicles (v), several spherical plastids (arrows) and lipoprotein droplets (l) (Bar = 10 μm). **B**. High magnification TEM showing a surface structure comprised of multiple concentric membranes. This structure is embedded within a thin epiplasm (arrowheads) that subtends the inner alveolar membrane (arrow); note that the outer alveolar membrane and plasma membrane are absent due to fixation artifact (Bar = 0.2 μm). **C**. High magnification TEM of a multiple-membrane bound structure that has pierced the epiplasm (arrow) (Bar = 0.2 μm). **D**. TEM of the pusule showing spherical vesicles surrounded by a double membrane (arrowheads) budding from the main "wall" of the chamber (arrow) (Bar = 1 μm). **E**. TEM through the sulcus showing the opening of the pusule, a flagellum (arrow) and a single row of microtubules (arrowheads) beneath the deepest alveolar membrane (Bar = 1 μm). Inset: Higher magnification view of the microtubules (see **E** for scale).

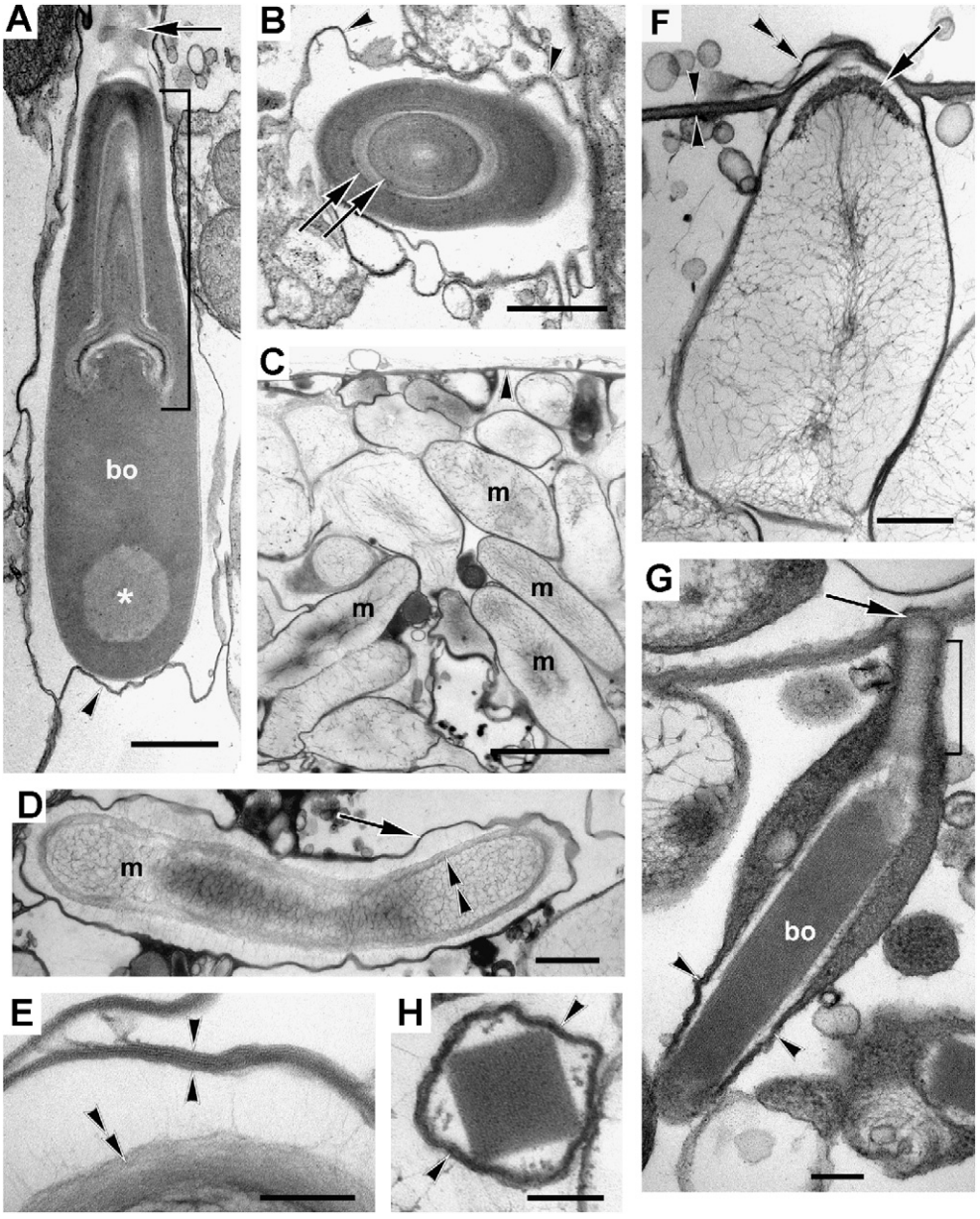

Figure 5. Transmission electron micrographs (TEM) of *Polykrikos lebourae* showing the organization and diversity of three types of extrusomes. **A**. TEM through the longitudinal axis of a taeniocyst showing the densely stained body (bo), a posterior amorphous zone (asterisk), a conical neck (bracket), an apical head (arrow) and the enveloping membrane (arrowhead) (Bar = 0.5 μm). **B**. Transverse TEM through the neck region of a taeniocyst showing the enveloping membrane (arrowheads) and the concentric lamellae (arrows) within the darkly stained body (Bar = 0.5 μm). **C**. Low magnification TEM showing a dense accumulation of mucocysts (m) beneath the alveolar membranes (arrowhead) (Bar = 2 μm). **D**. High magnification TEM of a vermiform mucocyst (m) showing a dense outer layer (arrowhead) around a fibrillar inner core. The entire mucocyst is surrounded by a continuous set of membranes (arrow) (Bar = 0.5 μm). **E**. High magnification TEM showing the set of 4—6 compressed membranes (arrows) that surround the mucocysts (m) (Bar = 0.2 μm). **F**. High magnification TEM of a mucocyst showing the fibrillar inner core and the dense apical 'cap' (arrow) protruding through the epiplasm (arrowheads) and remnants of the alveolar membranes (double arrowheads) (Bar = 0.25 μm). **G**. High magnification TEM of a trichocyst showing an enveloping membrane (arrowheads), an apical 'cap' (arrow), a neck comprised of small regularly arranged knobs (bracket) and a column-like body with a lattice-like structure (bo) (Bar = 0.2 μm). **H**. High magnification TEM of a trichocyst in transverse section showing the enveloping membrane (arrowheads) around the quadrangular shaped body (Bar = 0.2 μm).

arranged knobs, and an apical 'cap' (Fig. 5 G, 5 H). The trichocyst body had a quadrangular shape in transverse section (Fig. 5 H). In dense areas of the cytoplasm, endoplasmic reticulum and numerous small vacuoles of varying size were observed (Fig. 6 A). Putative peroxisomes (i.e. microbodies) were present (Fig. 6 B). Mitochondria contained tubular cristae and sometimes had circular inclusions formed from double membranes (Fig. 6 D, 6 E). The nuclei contained permanently condensed chromosomes (Fig. 6 F, 6 H), and the nuclear envelope had vesicular nuclear chambers (Fig. 6 F) with many close-set circular openings containing a central granule (Fig. 6 E, 6 F). Densely stained, amorphous material was present within the nucleolus (Fig. 6 G), and a large cavity within the nucleus was sometimes present (Fig. 6 G, 6 H).

The spherical plastids of *P. lebourae* had an aberrant ultrastructure (Fig. 7 A—F). The plastids always appeared circular in the TEM profiles, never fusiform (Fig. 7 A—C), and the thylakoid stacks showed an undulating pattern (Fig. 7 A—D). Thylakoids were always arranged in stacks of two (Fig. 7 D—F) and no girdle lamella was present. The thylakoid compartments were interrupted by large swellings (Fig. 7 D). These swellings could represent novel structures or a manifestation of artifacts caused by a suboptimal fixation of highly vacuolated cells. The round central structures within the plastids that were void of thylakoids are interpreted to be 'pyrenoids'. In addition, there were other thylakoid-free regions in the plastids that were different in position and composition to the pyrenoids (Fig. 7 B, 7 C). The pyrenoids had an electron-dense core (Fig. 7 B), which could represent plastid DNA. Plastid division was evident (Fig. 7 A), and the plastid envelope appeared to consist of two membranes (Fig. 7 E, 7 F). A vacuolar membrane surrounding several plastids was not observed. However, interpretations of membrane organization within the cell were difficult because of the highly vacuolated cytoplasm.

The photosynthetic form of *P. lebourae* swam in a straight line and rotated around its longitudinal axis. The pseudocolonies could also rotate quickly around a stationary point. Inactive pseudocolonies were sometimes embedded within a hyaline cyst (not shown), and in most cases, the cyst was eventually discarded and normal activity was regained. In one instance, we observed division of a pseudocolony within a hyaline cyst (not shown). Resting cyst production was not observed. Attempts to culture the photosynthetic form of *P. lebourae* were unsuccessful, which might indicate an obligate mixotrophic mode of feeding.

Morphology of the Heterotrophic Form of '*Polykrikos lebourae*'

Pseudocolonies of the heterotrophic form of '*P. lebourae*' (from Canadian and German sites) almost always consisted of eight zooids and two nuclei (Fig. 8 A—E); in Canada reduced pseudocolonies consisting of five or four zooids and one nucleus, containing nematocysts were also observed (Fig. 8 F—H). Specimens with eight zooids were 40.0—80.0 μm long and 30.0—50.0 μm wide in Canada, and 45.0—90.0 μm long and 32.5—55.0 μm wide in Germany, and lacked visible borders between zooids (Fig. 8 A). The cells were ovate in shape, with the terminal zooids being about half as wide as the central ones and the apical zooid having a pointing shape (Fig. 8 A—E). The acrobase was loop-shaped (Fig. 8 B). The pseudocolonies were obliquely flattened, and fused sulci were positioned laterally on the right-hand side of the cell (Fig. 8 C, 8 D). The cinguli were descending, displaced about one cingular width (Fig. 8 C—E). Eight sets of longitudinal and transverse flagella were present (Fig. 8 A, 8 D). The two nuclei were nearly spherical and were distributed within the anterior and posterior halves of the pseudocolony (Fig. 8 B).

The heterotrophic form of '*P. lebourae*' possessed taeniocyst-nematocyst-complexes typical for *Polykrikos* species (Fig. 8 C—E). A taeniocyst, associated with a nematocyst, anchored beneath the sulcus near each flagellar insertion zone (Fig. 8 C, 8 E). These complex extrusomes were also present in other parts of the pseudocolony (Fig. 8 C—E). Specimens contained yellow, orange, red and colorless food bodies of variable number and size, and positioned in different areas of the pseudocolony (Fig. 8 C). Many colorless granules were also present in the cytoplasm. Pseudocolonies of the heterotrophic form of '*P. lebourae*' swam in a straight line and rotated around its longitudinal axis. Vegetative or resting cysts were not observed.

Molecular Phylogeny of Polykrikoids

We generated two new SSU rDNA sequences from a natural population of the heterotrophic form of '*P. lebourae*' (syn.: *Polykrikos herdmanae* n. sp., see below) and two additional SSU rDNA

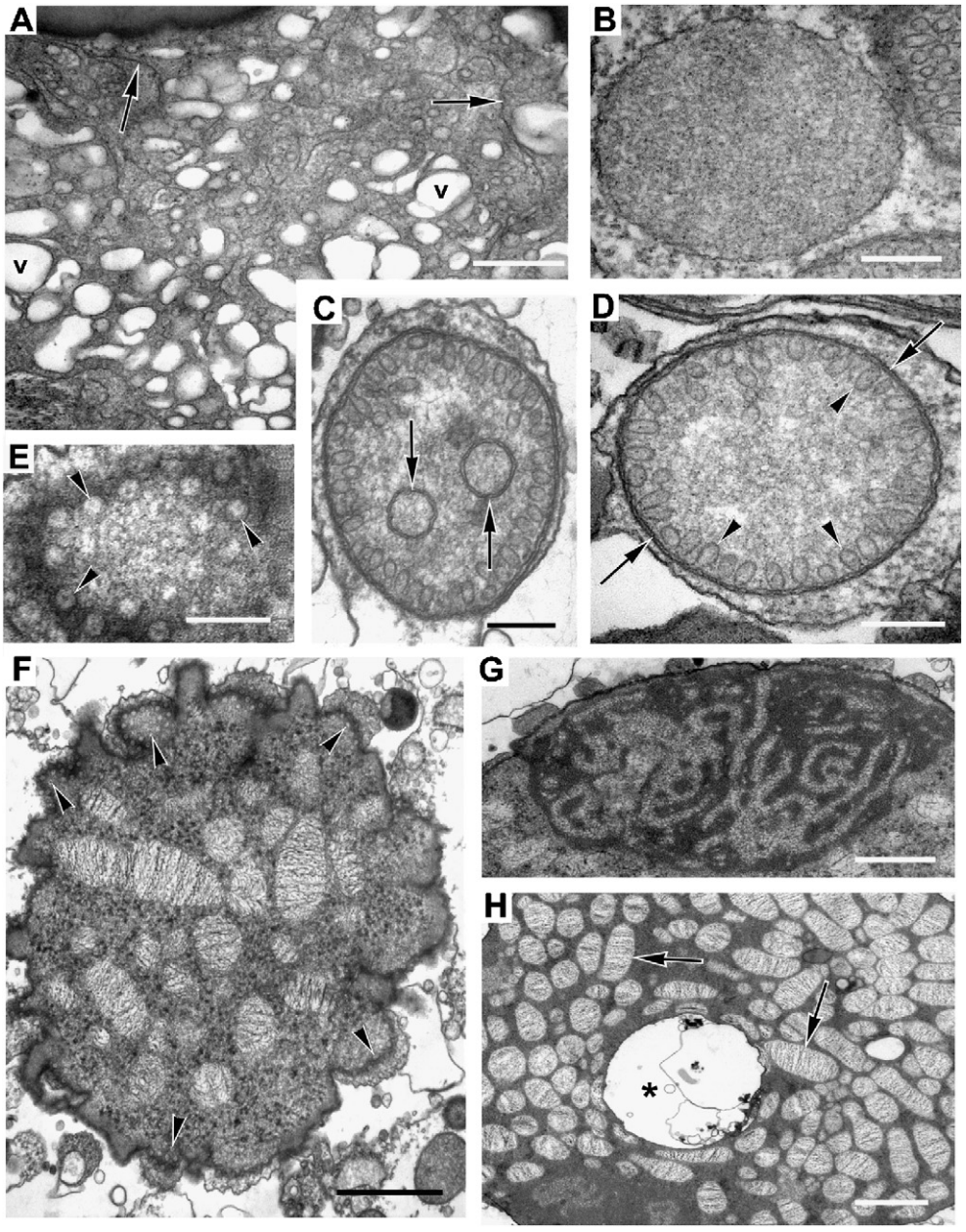

Figure 6. Transmission electron micrographs (TEM) of *Polykrikos lebourae* showing the ultrastructure of the nucleus, mitochondria and related organelles. **A**. TEM showing a dense area of cytoplasm with numerous vacuoles of varying size (v) and endoplasmic reticulum (arrows) (Bar = 0.5 μm). **B**. A putative peroxisome or microbody (bar = 0.3 μm). **C**. TEM of a mitochondrion showing two circular inclusions (arrows) formed from double membranes (Bar = 0.3 μm). **D**. TEM of a mitochondrion showing the enveloping double membrane (arrow) and a superficial distribution of tubular cristae (arrowheads) (Bar = 0.3 μm). **E—F**. Tangential TEMs through the nucleus showing the presence of nuclear chambers and the close-set distribution of nuclear pores, with central granule, in the nuclear envelope (arrowheads) (**E**, Bar = 0.2 μm; **F**, Bar = 1.5 μm). **G**. TEM showing a distinctive pattern of densely stained material within the nucleolus (Bar = 1.5 μm). **H**. TEM through the nucleus showing the permanently condensed chromosomes (arrows) and a large nuclear cavity (asterisk) (Bar = 2 μm).

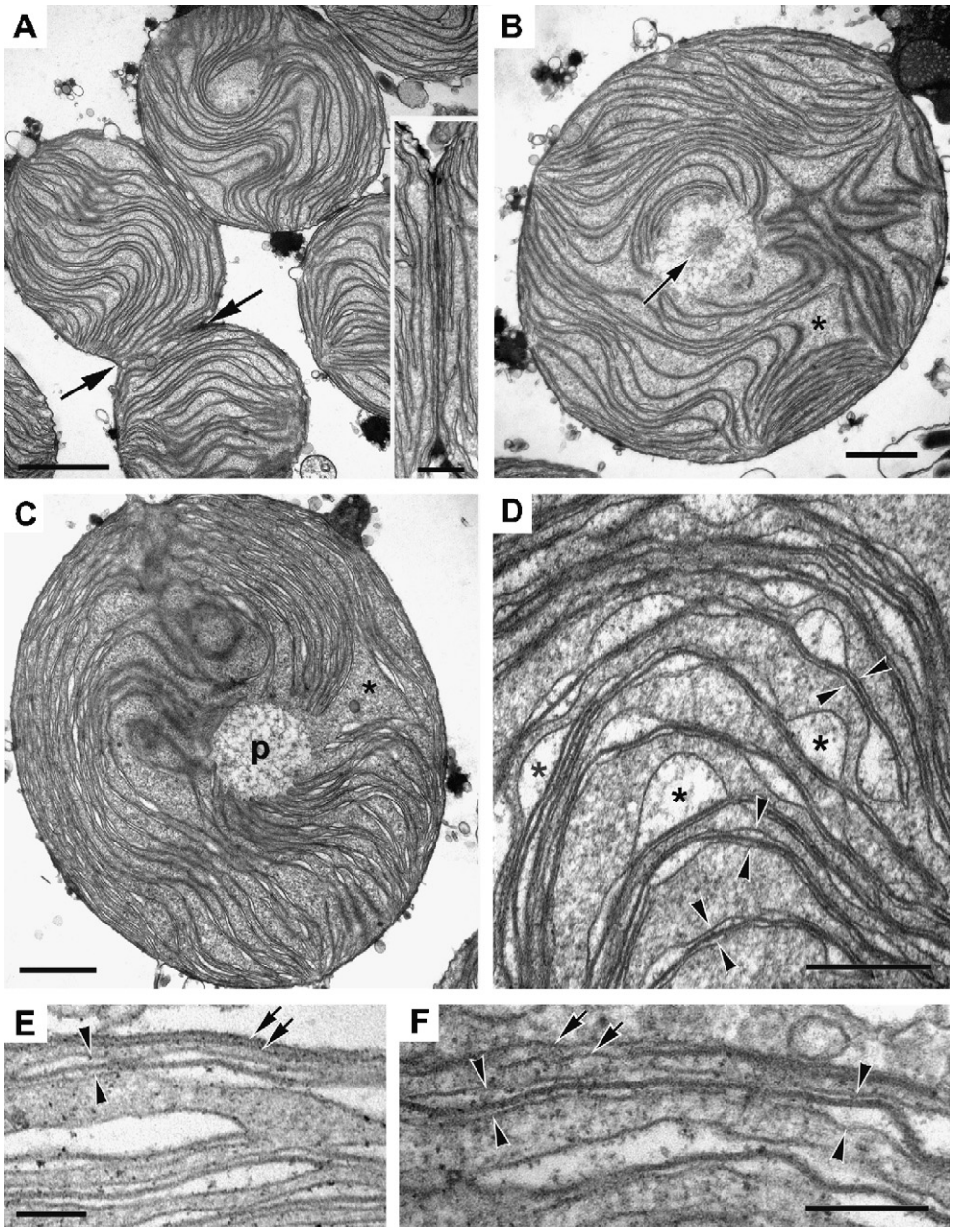

Figure 7. Transmission electron micrographs (TEM) of *Polykrikos lebourae* showing the aberrant ultrastructure of the plastids. **A**. Low magnification TEM showing the undulating pattern of thylakoid stacks and the division of adjacent plastids (arrows) (Bar = 2 μm). Inset: Higher magnification view of the plastid division plane (Bar = 0.5 μm). **B—C**. TEMs of whole plastids showing circular profiles, undulating pattern of thylakoid stacks, thylakoid-free regions (asterisks) and the electron-dense core (arrow) of centrally positioned pyrenoids (p) (Bars = 1 μm). **D**. High magnification TEM showing thylakoids arranged in pairs, which is evident by the repeating pattern of densely stained membranes 'thin—thick—thin' (between arrowheads). The thylakoid compartments are interrupted by large swellings (asterisks) (Bar = 0.3 μm). **E—F**. High magnification TEMs of the plastid surface showing thylakoids arranged in pairs (between arrowheads) and two enveloping membranes (arrows) (**E**, Bar = 0.1 μm; **F**, Bar = 0.2 μm).

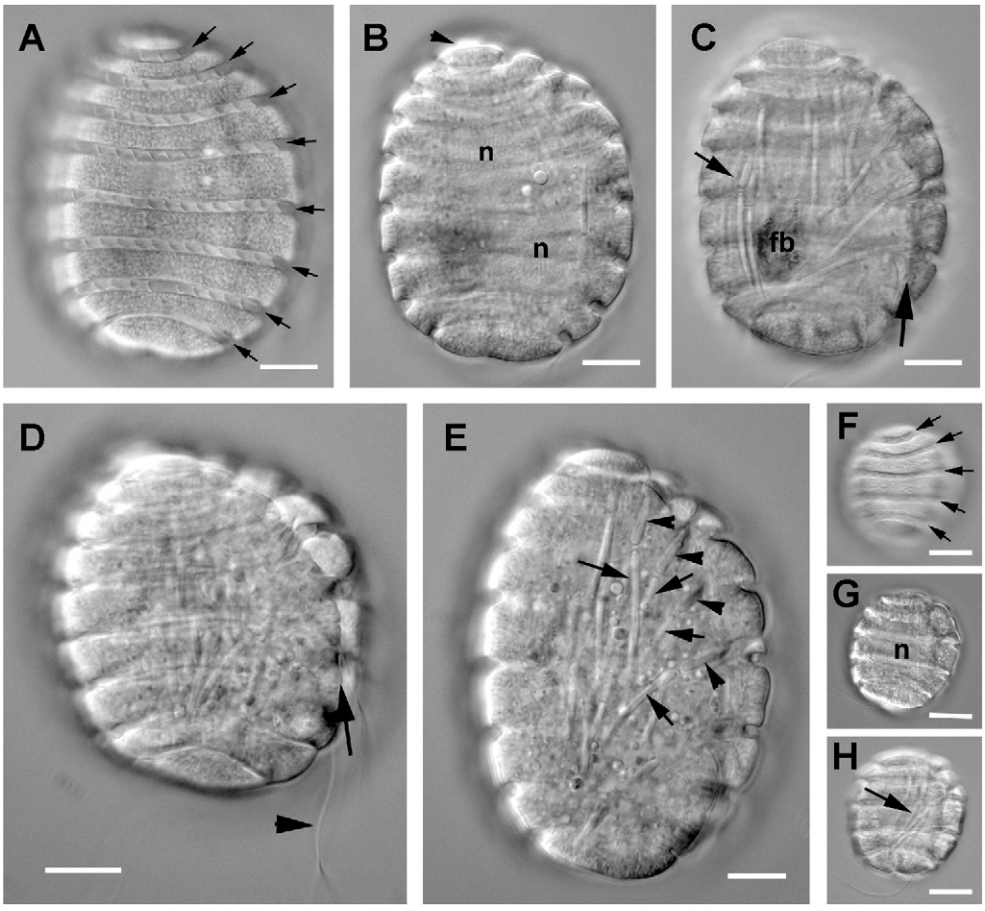

Figure 8. Light micrographs (LM) of *Polykrikos herdmanae* n. sp. **A.** Pseudocolony in focus on the eight transverse flagella within the cinguli (arrows). **B.** Pseudocolony showing the relative positions of two nuclei (n) and the acrobase (arrowhead). **C.** Distribution of taeniocyst—nematocyst complexes (e.g. arrow), presence of a food body (fb), and the position of the fused sulci (large arrow). **D.** Pseudocolony showing the position of the fused sulci (arrow) and a longitudinal flagellum (arrowhead). **E.** Pseudocolony containing taeniocyst—nematocyst complexes positioned at the flagellar insertion zones in the sulcus. Note the taeniocyst (arrowheads) and nematocyst (arrows) positions in the complexes. **F.** Aberrant pseudocolony consisting of five zooids. Note the five cinguli (arrows). **G.** Same pseudocolony as in Figure F containing one nucleus (n). **H**. Same pseudocolony as in Figure F containing taeniocyst-nematocyst complexes (arrow). (**A—H**, Bar = 10 μm).

sequences from the photosynthetic form of *P. lebourae* (from a natural population collected in 2006). The phylogenetic position of these sequences within the dinoflagellate clade was analyzed with a 40-taxon alignment consisting mainly of athecate taxa representing all known clades in the Gymnodiniales (1696 unambiguously aligned base positions); a previously published sequence from the photosynthetic form of *P. lebourae*, collected in 2005, was also included (Hoppenrath and Leander 2007) (Fig. 9). The inferred phylogenetic framework demonstrated strong support for the *Gymnodinium s.s.* clade. The type species of *Gymnodinium*, namely *Gymnodinium fuscum* (Ehrenberg) Stein, formed the sister lineage to a robust '*Polykrikos*' clade, albeit with only modest statistical support (Fig. 9). The '*Polykrikos*' clade consisted of *Pheopolykrikos hartmannii*, *Polykrikos kofoidii*, the photosynthetic form of *P. lebourae* and the heterotrophic form of '*P. lebourae*'. The sequences from the heterotrophic form of '*P. lebourae*' (shown as *Polykrikos herdmanae* n. sp.) formed a robust clade that was distinct from a robustly supported clade of sequences derived from two independent samples of the photosynthetic form of *P. lebourae*, each taken in different years (Fig. 9). A more inclusive clade consisting of all of the sequences

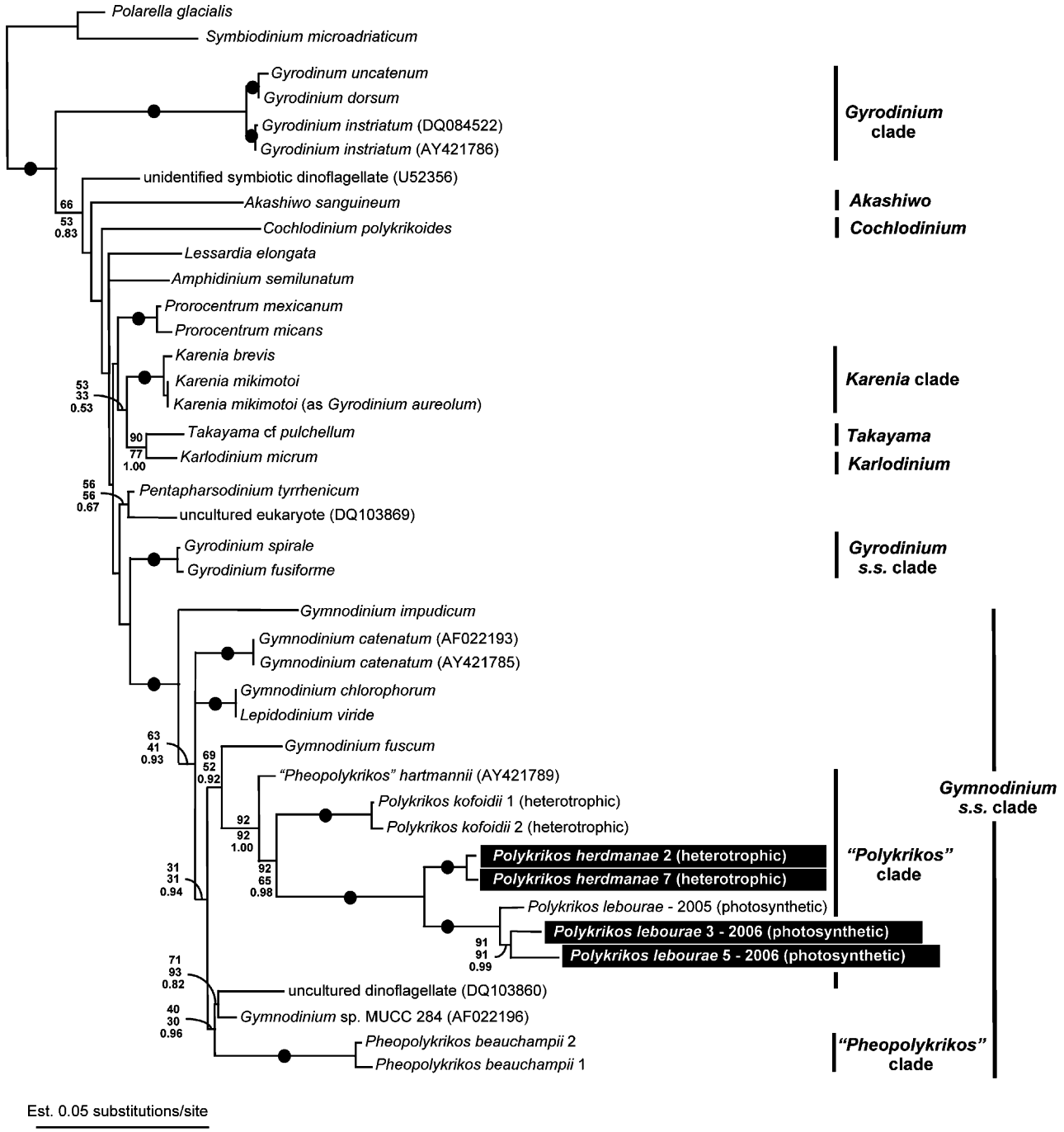

Figure 9. Gamma-corrected maximum likelihood tree ($-\ln L = 7415.3125$, $\alpha = 0.19$, proportion of invariable sites $= 0.1$, 8 rate categories) inferred using the GTR model of substitution on an alignment of 40 SSU rDNA sequences and 1696 unambiguously aligned sites. Numbers at the branches denote bootstrap percentages using maximum likelihood — HKY (top), bootstrap percentages using weighted neighbor-joining (middle) and Bayesian posterior probabilities — GTR (bottom). Black dots on branches denote robust bootstrap percentages and posterior probabilities of 95% or higher. The sequences derived from this study are highlighted in the shaded boxes.

derived from both the photosynthetic and heterotrophic form of '*P. lebourae*' was strongly supported by the data (Fig. 9). This clade, containing benthic species with eight zooids and two nuclei per pseudocolony, was the sister group to *Polykrikos kofoidii*, which is a heterotrophic species found in planktonic environments and consisting of four zooids and two nuclei per pseudocolony. The clade consisting of *P. kofoidii* and both forms of '*P. lebourae*' was the sister group to *Pheopolykrikos hartmannii*, which is a photosynthetic species found in planktonic environments and consisting of two zooids and two nuclei per pseudocolony (Fig. 9). The photosynthetic *Pheopolykrikos beauchampii*, which consists of four nuclei and four zooids per pseudocolony, was nested within a group that was sister to the clade comprising *Gymnodinium fuscum* and the '*Polykrikos*' clade, albeit with very weak statistical support (Fig. 9).

Taxonomic Descriptions

Polykrikos herdmanae Hoppenrath et Leander n. sp.

Syn.: *Polykrikos schwartzii* partim, sensu Herdman 1922; *Polykrikos lebourae* partim, sensu Herdman 1923, sensu Lebour 1925, sensu Schiller 1933, sensu Baillie 1971.

Holotype: Fig. 8A—C (same specimen).

Type locality: Boundary Bay, British Columbia, Canada.

Etymology: In honor of E. C. Herdman, who first observed and described this heterotrophic taxon.

Diagnosis: Pseudocoloniae sine thecis consistentes plerumque ex octo zooidibus et duobus nucleis, sed aliquando minores pseudocoloniae consistentes ex quattuor aut quinque zooidibus et uno nucleo. Pseudocoloniae ovatae et oblique aequae pressae, habentes zooides terminales tantas dimidias longas quantas zooides medias. Pseudocoloniae consistentes ex octo zooidibus 40.0—90.0 μm longae et 30.0—55.0 μm altae. Termini non conspicui inter zooides. Acrobasis in formam laquei. Coniuncti sulci, lateraliter positi in dextra latere pseudocoloniae. Cinguli descendentes, circa latitudo unae cingulae loco moti. Flagellae in octo recemis dispositae et ex transverso et per longitudinem. Conformationes taeniocystes-nematocystes adsunt. Plastides desunt.

Athecate pseudocolonies usually consisting of eight zooids and two nuclei, but can also occur as reduced pseudocolonies consisting of five or four zooids and one nucleus. Pseudocolonies are ovate and obliquely flattened, with terminal zooids about half as wide as central zooids. Eight-zooid pseudocolonies are 40.0—90.0 μm long and 30.0—55.0 μm wide. No visible borders between zooids. Loop-shaped acrobase. Fused sulci, positioned laterally on the right-hand side of the pseudocolony. Descending cinguli, displaced about one cingular width. Eight sets of longitudinal and transverse flagella. Taeniocyst—nematocyst complexes present. Plastids absent.

Polykrikos lebourae Herdman emend. Hoppenrath et Leander, herein

Herdman 1923, Proc Trans Liverpool Biol Soc 37, p. 60, Fig. 6.

Syn.: *Polykrikos* sp.? sensu Herdman 1921, maybe *Polykrikos schwartzii* partim sensu Herdman 1922.

Citations: as *Polykrikos lebourae* in Lebour 1925, Schiller 1933, Balech 1956, Hulburt 1957, Dragesco 1965, Baillie 1971, Dodge 1982, 1989, Paulmier, 1992.

Description: Pseudocolonies consisting of eight zooids and two nuclei. Reduced pseudocolonies consisting of four zooids can occur. Eight-zooid pseudocolonies are 37.5—90.0 μm long and 20.0—50.0 μm wide. Pseudocolonies are ovate in shape and obliquely flattened, with terminal zooids about half as wide as central zooids. No visible borders between zooids. Loop-shaped acrobase. Fused sulci, positioned laterally on the right-hand side of the pseudocolony. Cinguli descending, displaced about one to two cingular widths. Eight sets of longitudinal and transverse flagella. Two nuclei. Many small, golden-brown, spherical or spindle-shaped plastids with central pyrenoid. Taeniocyst-nematocyst complexes sometimes present. Sometimes containing food bodies. Hyaline vegetative cysts.

Discussion

General Morphology and Taxonomy of Polykrikoids

All *Polykrikos* species have (1) a loop-shaped acrobase, (2) descending cinguli with the displacement being greatest in the most anterior zooid, (3) a slightly curved sulcus reaching the posterior end of the pseudocolony, (4) taeniocyst—nematocyst complexes, (5) half or a quarter the number of nuclei as zooids, and (6) the ability to disassemble into pseudocolonies with fewer zooids containing only one nucleus. *Polykrikos lebourae* and *P. herdmanae* n. sp. have strongly

laterally flattened pseudocolonies consisting of eight zooids and two nuclei with the terminal zooids being distinctly narrower than the intermediate zooids. This combination of features distinguishes them from all other polykrikoid dinoflagellates (table 1 in Hoppenrath and Leander 2007). The pseudocolonies of *Polykrikos schwartzii* consist of eight zooids and four nuclei; the pseudocolonies of *P. kofoidii* consist of four zooids and two nuclei. The pseudocolonies in both taxa are barrel-shaped (e.g., Nagai et al. 2002). The pseudocolonies of *Pheopolykrikos hartmannii* and *P. beauchampii* are photosynthetic and consist of the same number of nuclei as zooids, namely two and four respectively. The presence of complex extrusomes in these taxa is uncertain (Hoppenrath and Leander 2007). The morphological distinction between *P. lebourae* and *P. herdmanae* n. sp. is the presence of plastids in the former and the obvious and constant presence of canonical taeniocyst—nematocyst complexes in the latter. The interpretation that these morphological differences reflect the identity of two distinct species is supported by the molecular phylogenetic results shown in Figure 9 (i.e. significant and consistent differences in SSU rDNA gene sequences).

Because the original description of *P. lebourae* included both the photosynthetic and heterotrophic morphotypes (Herdman 1923), it was initially difficult to determine which morphotype should be described as new. In her first observation of the taxon, Herdman (1921) mentioned that, "'*Polykrikos* sp.?' occurred fairly regularly on certain parts of the shore though never in such abundance as to cause discoloration" (Herdman 1921, p. 61). Discolorations in the sediment can only be caused by photosynthetic species, and therefore we interpreted this statement as being related to the phototrophic morphotype of *P. lebourae*, even though the line drawing did not show plastids (Herdman 1921, p. 62; our Fig. 5). The taxon was then misidentified as *P. schwartzii* (Herdman 1922), and feeding behavior was described in what must have been a heterotrophic form. The most recent description of *P. lebourae* included both morphotypes (Herdman 1923), and it was explicitly stated by Herdman (1923, p. 60) that only one sand-dwelling species was observed over several years and her earlier observations on *P. schwartzii* were actually on *P. lebourae*. In light of this series of observations and of the fact that the species description lacked any mention of nematocysts (Herdman 1923, p. 60; our Fig. 1 E), which is a striking feature of the heterotrophic morphotype, we chose to describe the heterotrophic form as a new species and to amend the description of the photosynthetic form (see Results).

Comparative Ultrastructure of Polykrikoids

Polykrikos kofoidii and species of *Gymnodinium* s.s. share several distinctive features associated with the nuclear envelope, such as nuclear chambers with nuclear pores and a 'nuclear fibrillar connective' (Bradbury et al. 1983; Daugbjerg et al. 2000; Dodge and Crawford 1969; Hansen and Moestrup 2005; Hansen et al. 2000; Hoppenrath and Leander 2007). These shared morphological characters are consistent with the close relationships between *Polykrikos* and *Gymnodinium* s.s. in our molecular phylogenetic analyses (Fig. 9). The so-called 'double-layered fibrous nuclear cortex (capsule)' directly beneath the nuclear envelope in *P. kofoidii* does not appear to be present in other species of *Gymnodinium* s.s., including *P. lebourae* (Fig. 6 F), and so far is shared only with *Actiniscus pentasterias* (Bradbury et al. 1983; Hansen 1993). Nonetheless, like other members of the *Gymnodinium* s.s. clade (e.g. *Polykrikos kofoidii*, *Gymnodinium fuscum* and *Gymnodinium chlorophorum* Elbrächter et Schnepf; Hansen and Moestrup 2005; Hansen et al 2000), the nuclear envelope of *P. lebourae* has vesicular nuclear chambers with nuclear pores containing a central granule.

The pusule of *P. lebourae* is similar to that described for *Gymnodinium fuscum* (Dodge and Crawford 1969; Hansen et al. 2000) and *Gyrodinium spirale* (Bergh) Kofoid et Swezy (Hansen and Daugbjerg 2004). Mucocysts of the same form and cellular distribution also occur in all three species (Hansen and Daugbjerg 2004; Hansen et al. 2000). The ultrastructure and cellular position of the taeniocysts in *P. lebourae* were similar to those described in *P. schwartzii* (Greuet 1972) and *P. kofoidii* (Westfall et al. 1983). The absence of any previous reports that noticed complex extrusomes in *P. lebourae* probably reflects the obscuring effect caused by the dense distribution of plastids found in this lineage (Balech 1956; Dragesco 1965; Herdman 1923; Hoppenrath 2000).

The consistent presence of canonical taeniocyst—nematocyst complexes in *Polykrikos herdmanae* n. sp. (the former heterotrophic form of *P. lebourae*) and the occasional presence also in *P. lebourae* is a character shared with heterotrophic polykrikoids, namely *P. kofoidii* and *P. schwartzii*. These complex organelles are

unlikely to have evolved several times independently within one dinoflagellate clade, and we infer that their presence is a robust synapomorphy for the '*Polykrikos* clade' (Fig. 9). Although the original description of *Pheopolykrikos hartmannii* (Zimmermann 1930) mentions the presence of nematocysts, it remains to be unambiguously demon;strated whether *Pheopolykrikos hartmannii* actually possesses these complex extrusomes and, like in *P. lebourae*, whether taeniocyst—nematocyst complexes were simply overlooked in subsequent light microscopical observations (Hulburt 1957; Matsuoka and Fukuyo 1986).

Another solid, but unanticipated, synapomorphy for the '*Polykrikos* clade' is the presence of two nuclei within one cytoplasm, irrespective of zooid number (Hoppenrath and Leander 2007). *Polykrikos lebourae* and *P. herdmanae* illustrate the most extreme condition within the group, having pseudcolonies consisting of eight tightly integrated zooids and two nuclei.

Comparative Ultrastructure of the Plastids in *Polykrikos lebourae*

Polykrikos lebourae is the only described *Polykrikos* species known to be photosynthetic. Although one report indicated that *P. schwartzii* could sometimes be photosynthetic as well (Matsuoka and Fukuyo 1986, p. 815), this claim was never demonstrated and we suspect that it is a misinterpretation (Hoppenrath and Leander 2007). Both species of *Pheopolykrikos*, namely *P. beauchampii* and *P. hartmannii*, are photosynthetic, but ultrastructural and biochemical characteristics of their plastids are not known (Chatton 1933; Hulburt 1957; Matsuoka and Fukuyo 1986; Zimmermann 1930). Most likely, species of *Pheopolykrikos* have the usual peridinin-containing dinoflagellate plastids, like those described for the closely related *Gymnodinium fuscum* (Dodge and Crawford 1969; Hansen et al. 2000), but this remains to be demonstrated. The usual peridinin-containing dinoflagellate plastids consist of a triple membrane envelope, with no ribosomes associated with the outermost membrane or connections to the thylakoids (Dodge 1975, Schnepf and Elbrächter 1999). Moreover, a girdle lamella is generally absent, pyrenoids are sometimes present and thylakoids generally occur in stacks of three (Dodge 1975; Dodge and Crawford 1971; Schnepf and Elbrächter 1999).

The plastids of *P. lebourae* have the same yellow-brown color as those found in the peridinin-containing plastids of other dinoflagellates and in diatoms. Dinoflagellates harboring diatom plastids are known in *Durinskia baltica* (Levander) Carty et Cox (syn.: *Glenodinium balticum* Levander, *Peridinium balticum* (Levander) Lemmermann), *Kryptoperidinium foliaceum* (Stein) Lindemann (syn.: *Peridinium foliaceum* Stein, *Glenodinium foliaceum* Stein), *Peridinium quinquecorne* Abé, *Gymnodinium quadrilobatum* Horiguchi et Pienaar and *Galeidinium rugatum* Tamura et Horiguchi (Dodge and Crawford 1971; Horiguchi and Pienaar 1991, 1994; Tamura et al. 2005; Tomas and Cox 1973). Except for *K. foliaceum*, all of these species occur in benthic habitats, like *P. lebourae*. The diatom-derived plastids of these dinoflagellates have thylakoids in stacks of three and a girdle lamella, and they reside within nearly intact endosymbionts that still contain the diatom nucleus (Schnepf and Elbrächter 1999). All of these species still contain a reduced dinoflagellate plastid in the form of a stigma, which functions in phototaxis.

By contrast, *P. lebourae* lacks a stigma and possesses plastids with (putatively) only two enveloping membranes, thylakoids in stacks of two and central pyrenoids devoid of thylakoids. This unusual plastid ultrastructure and the close phylogenetic relationship of *P. lebourae* to several heterotrophic species, namely *P. kofoidii and P. herdmanae*, suggest that photosynthesis in *P. lebourae* might be a derived state for this lineage. In other words, it is plausible that the plastids in *P. lebourae* are not vertically homologous to the peridinin-containing plastids of other dinoflagellates, and instead evolved via a separate endosymbiotic acquisition following the reduction or loss of the peridinin-containing plastids of its distant, *Gymnodinium*-like ancestors. The loss and replacement of plastids is not unusual in dinoflagellates; it appears to have happened several times independently within the group (Saldarriaga et al. 2001, 2004; Shalchian-Tabrizi et al. 2006; Taylor 2004). Kleptoplastidy could also explain the presence of plastids in *P. lebourae*. We observed stages that resemble plastid division within the pseudocolony and did not observe any evidence that would be indicative of a food vacuole, such as a continuous membrane around several plastids, which points against kleptoplastidy. However, not all kleptoplastids in dinoflagellates seem to be necessarily surrounded with a food vacuole (Koike et al. 2005). Our results cannot definitively determine whether the plastids are established or transient.

Like in *P. lebourae*, some dinoflagellate plastids have been recorded with an envelope of only two membranes and occasionally thylakoids in stacks of two, such as *Prorocentrum mariae-lebouriae* (Schnepf and Elbrächter 1999). The plastids in *Dinophysis* also have pairs of thylakoids and are bounded by only two membranes (Schnepf and Elbrächter 1988). However, the thylakoid lumen in this lineage is filled with electron-dense phycoerythrin (a reddish color), and the plastid is of cryptophyte origin (Schnepf and Elbrächter 1988, 1999). Plastids derived from prasinophytes have been demonstrated in *Gymnodinium chlorophorum* Elbrächter et Schnepf and *Lepidodinium viride* Watanabe, Suda, Inouye, Sawaguchi et Chihara (Elbrächter and Schnepf 1996; Shalchian-Tabrizi et al. 2006; Watanabe et al. 1991). These plastids also have two outer membranes and thylakoids in stacks of two or three, but they have a composition of pigment that makes them appear green. Several dinoflagellate species also contain prymnesiophycean-, chrysophycean- or dictyochophycean-like plastids, but they differ significantly in morphology to the one described here for *P. lebourae* (see Schnepf and Elbrächter 1999; Schweikert and Elbrächter 2004).

There are also similarities between the plastids in *P. lebourae* and the retinal bodies of ocelloids in warnowiid dinoflagellates (Greuet 1987). On strictly morphological grounds, warnowiids appear to be closely related to polykrikoids and other members of the *Gymnodinium* s.s., and this hypothesis is supported by preliminary molecular phylogenetic results (Hoppenrath and Leander, unpublished data). Ultrastructural studies of dividing cells indicate that the retinal bodies of warnowiid ocelloids appear to be highly derived plastids consisting of thylakoids in stacks of two and an enveloping membrane(s) (Greuet 1987). Although speculative, it is possible that the aberrant ultrastructural similarities between the plastids of *P. lebourae* and warnowiid retinal bodies are homologous. Molecular phylogenetic markers from the plastid genome in *P. lebourae* would help unambiguously determine their relationship to other lineages of plastids in eukaryotes. Because attempts to culture *P. lebourae* were unsuccessful, this avenue of investigation was beyond the scope of this particular study.

Methods

Organisms and light microscopy: Sand samples containing *Polykrikos lebourae* were collected with a spoon during low tide at Centennial Beach, Boundary Bay, BC, Canada during the summer and fall months of 2005 and 2006. *Polykrikos herdmanae* n. sp. occurred at the same site in May of 2006 together with *P. lebourae*. The sand samples were transported directly to the laboratory, and the flagellates were separated from the sand by extraction through a fine filter (mesh size 45 μm) using melting seawater-ice (Uhlig 1964). The flagellates accumulated in a Petri dish beneath the filter and were then identified at 40 to 250 × magnifications. Cells were isolated by micropipetting for the preparations described below.

Pseudocolonies were observed directly and micromanipulated with a Leica DMIL inverted microscope connected to a PixeLink Megapixel color digital camera. For differential interference contrast (DIC) light microscopy, micropipetted cells were placed on a glass specimen slide and covered with a cover slip. Images were produced with a Zeiss Axioplan 2 imaging microscope connected to a Leica DC500 color digital camera.

Observations made earlier in the North German Wadden Sea, obtained by the same methodology (Hoppenrath 2000), were also considered.

Scanning electron microscopy: A mixed-extraction sample containing *P. lebourae* was fixed with OsO_4 for 30 min at room temperature. Cells were transferred onto a 5-μm polycarbonate membrane filter (Corning Separations Div., Acton, MA), washed with distilled water, dehydrated with a graded series of ethanol and 100% hexamethyldisilazane (HMDS) at the end, and air dried. Filters were mounted on stubs, sputter-coated with gold and viewed under a Hitachi S4700 Scanning Electron Microscope. Some SEM images were presented on a black background using Adobe Photoshop 6.0 (Adobe Systems, San Jose, CA).

Transmission electron microscopy: Pseudocolonies were concentrated in an Eppendorf tube by micropipetting and slow centrifugation. The pellet of cells was prefixed with 2% (v/v) glutaraldehyde (in unbuffered seawater) at 4 °C for 30 min. Cells were washed twice in filtered seawater before post-fixation in 1% (w/v) OsO_4 (in unbuffered seawater) for 30 min at room temperature. Cells were dehydrated through a graded series of ethanol, infiltrated with acetone—resin mixtures (acetone, 2:1, 1:1, 1:2, Epon 812 resin) and embedded in Epon 812 resin. The block was polymerized at 60 °C and sectioned with a diamond knife on a Leica Ultracut UltraMicrotome. Thin sections were post-stained with uranyl acetate and lead citrate and viewed under a Hitachi H7600 Transmission Electron Microscope.

DNA extraction, PCR amplification, alignment and phylogenetic analysis: Eight individual pseudocolonies of the heterotrophic *Polykrikos herdmanae* n. sp. were isolated from a natural population, washed three times in filtered (eukaryote-free) seawater and deposited in a 1.5 ml Eppendorph tube. Eleven individually isolated pseudocolonies of the phototrophic *P. lebourae* were treated in the same way. Genomic DNA was extracted by placing washed pseudocolonies in distilled water that was directly used for PCR. The PCR amplification protocol using universal eukaryotic primers, reported previously (Leander et al. 2003), consisted of an initial denaturing period (95 °C for 2 min); 35 cycles of denaturing (92 °C for 45 s), annealing (48 or 50 °C for 45 s), and extension (72 °C for 1.5 min); and a final extension period (72 °C for 5 min). PCR products corresponding to the expected size were gel isolated and cloned into the pCR2.1 using the TOPO TA cloning kit (Invitrogen). New sequences from *Polykrikos herdmanae* and *P. lebourae* were completely sequenced with ABI big-dye reaction mix using both vector primers and two internal primers oriented in both directions (GenBank accession codes DQ822481, DQ975470—DQ975472).

The SSU rDNA sequences (two different clones from each species; a total of four new sequences) were aligned with other alveolate sequences using MacClade 4 (Maddison and Maddison 2000), forming a 40-taxon alignment. Because the backbone of overall dinoflagellate phylogeny is poorly resolved (see Hoppenrath and Leander 2007), outgroup selection for the *Gymnodinium* s.s. clade was somewhat arbitrary. Our main concerns in chosing our taxon sample were to ensure that (1) all known clades of the Gymnodiniales were represented and (2) the outgroup taxa (e.g. *Polarella* and *Symbiodinium*) did not represent unusually long branches. The alignment is available on request from the authors.

Maximum likelihood (ML), ML-distance and Bayesian methods under different DNA substitution models were performed. All gaps were excluded from the alignments prior to phylogenetic analysis. The alpha shape parameters were estimated from the data using the Hasegawa—Kishino—Yano model for base substitutions (HKY), a gamma distribution with invariable sites and eight rate categories, respectively (40-taxon alignment: $\alpha = 0.19$, Ti/Tv $= 2.42$, $i = 0.1$). Gamma-corrected ML trees (analyzed using the parameters listed above) were constructed with PAUP* 4.0 using HKY and the general time reversible (GTR) model for base substitutions (Posada and Crandall 1998; Swofford 1999). Gamma corrected ML tree topologies found with HKY and GTR were identical. ML bootstrap analyses were performed on the 40-taxon alignment with PAUP* 4.0 (Swofford 1999) on one hundred re-sampled data sets using HKY and the alpha shape parameter and transition/transversion ratio (Ti/Tv) estimated from the original data set. ML bootstrap analyses were done using HKY (rather than GTR) in order to help reduce the computational burden required.

ML distances were calculated with TREE-PUZZLE 5.0 using the HKY substitution matrix (Strimmer and Von Haeseler 1996). A distance tree was constructed with weighted neighbor joining (WNJ) using Weighbor (Bruno et al. 2000). Five hundred bootstrap data sets were generated with SEQBOOT (Felsenstein 1993). Respective distances were calculated with the shell script 'puzzleboot' (M. Holder and A. Roger, www.tree-puzzle.de) using the alpha shape parameter and transition/transversion ratios estimated from the original dataset and analyzed with Weighbor.

We also examined the SSU rDNA data set with Bayesian analysis using the program MrBayes 3.0 (Huelsenbeck and Ronquist 2001). The program was set to operate with GTR, a gamma distribution and four Monte—Carlo—Markov chains (MCMC) (default temperature $= 0.2$). A total of 2,000,000 generations were calculated with trees sampled every 100 generations and with a prior burn-in of 200,000 generations (2000 sampled trees were discarded). A majority rule consensus tree was constructed from 18,000 post-burn-in trees with PAUP* 4.0. Posterior probabilities correspond to the frequency at which a given node is found in the post-burn-in trees.

GenBank accession numbers: (AF276818) *Akashiwo sanguinea*, (AF069516) (AF274256) *Amphidinium semilunatum*, (AY421781) *Cochlodinium polykrikoides*, (AF022193) *Gymnodinium catenatum*, (AY421785) *Gymnodinium catenatum*, (AM184122) *Gymnodinium chlorophorum*, (AF022194) *Gymnodinium fuscum*, (AF022197) *Gymnodinium impudicum*, (AF022196) *Gymnodinium* sp. MUCC 284, (AF274261) *Gyrodinium dorsum*, (AB120002) *Gyrodinium fusiforme*, (AY421786) *Gyrodinium instriatum*, (DQ084522) *Gyrodinium instriatum*, (AB120001) *Gyrodinium spirale*, (AF274263) *Gyrodinium uncatenum*, (AF274259) *Karenia brevis*, (AF009131) *Karenia mikimotoi*, (AJ415517) *Karenia mikimotoi* (as *Gyrodinium aureolum*), (AF274262) *Karlodinium micrum*, (AF022199) *Lepidodinium viride*, (AF521100) *Lessardia elongata*, (AF02220) *Pentapharsodinium*

tyrrhenicum, (DQ371294, DQ371295) *Pheopolykrikos beauchampii*, (AY421789) *Pheopolykrikos hartmannii*, (AF099183) *Polarella glacialis*, (DQ371291, DQ371292) *Polykrikos kofoidii*, (DQ371293) *Polykrikos lebourae*, (DQ822481) *Polykrikos herdmanae*, (Y16232) *Prorocentrum mexicanum*, (M14649) *Prorocentrum micans*, (M88521) *Symbiodinium microadriaticum*, (AY800130) *Takayama cf pulchellum*, (DQ103860) uncultured eukaryote, (DQ103869) uncultured eukaryote, (U52356) unidentified symbiotic dinoflagellate.

Acknowledgements

We would like to thank S. Sparmann, a recipient of an NSERC Undergraduate Student Research Award, for sampling in 2006 and for taking some LM images of *P. lebourae* (Fig. 2 D—G). We are also grateful to T. Deline, University of British Columbia, for assisting us with the Latin diagnosis, and M. Schweikert, University of Stuttgart, for discussions on the comparative ultrastructure of plastids. This work was supported by a scholarship to M. Hoppenrath from the Deutsche Forschungsgemeinschaft (Grant Ho3267/1-1) and by grants to B. S. Leander from the National Science and Engineering Research Council of Canada (NSERC 283091-04) and the Canadian Institute for Advanced Research, Program in Evolutionary Biology.

References

Balech E (1956) Étude des dinoflagellés du sable de Roscoff. Rev Algol **2**: 29—52

Baillie KD (1971) A Taxonomic and Ecological Study of Intertidal Sand-Dwelling Dinoflagellates of the North Eastern Pacific Ocean, MS thesis. University of British Columbia, Vancouver, 110pp

Bradbury PC, Westfall JA, Townsend JW (1983) Ultrastructure of the dinoflagellate *Polykrikos*. II. The nucleus and its connections to the flagellar apparatus. J Ultrastruct Res **85**: 24—32

Bruno WJ, Socci ND, Halpern AL (2000) Weighted neighbor joining: a likelihood-based approach to distance-based phylogeny reconstruction. Mol Biol Evol **17**: 189—197

Chatton É (1914) Les cnidocystes du Péridinien *Polykrikos schwartzii* Bütschli. Arch Zool Exp et Gen **54**: 157—194

Chatton É (1933) *Pheopolykrikos beauchampi* nov. gen., nov. sp., dinoflagellé polydinide autotrophe, dans l'Étang de Thau. Bull Soc Zool Fr **58**: 251—254

Chatton É, Grassé PP (1929) Le chondriome, le vacuome, les vésicules osmiophiles, le parabasal, les trichocystes et les cnidocystes du Dinoflagellé *Polykrikos schwartzii* Bütschli. C R Soc Biol C **C**:281—284

Daugbjerg N, Hansen G, Larsen J, Moestrup Ø (2000) Phylogeny of some of the major genera of dinoflagellates based on ultrastructure and partial LSU rDNA sequence data, including the erection of three new genera of unarmoured dinoflagellates. Phycologia **39**: 302—317

Dodge JD (1975) A survey of chloroplast ultrastructure in the Dinophyceae. Phycologia **14**: 253—263

Dodge JD (1982) Marine Dinoflagellates of the British Isles. Her Majesty's Stationery Office, London, 303pp

Dodge JD (1989) Records of marine dinoflagellates from North Sutherland (Scotland). Br phycol J **24**: 385—389

Dodge JD, Crawford RM (1969) The fine structure of *Gymnodinium fuscum* (Dinophyceae). New Phytol **68**: 613—618

Dodge JD, Crawford RM (1971) A fine-structural survey of dinoflagellate pyrenoids and food-reserves. Bot J Linn Soc **64**: 105—115

Dragesco J (1965) Étude cytologique de quelques flagellés mésopsammiques. Cahiers Biol Mar **6**: 83—115

Elbrächter M, Schnepf E (1996) *Gymnodinium chlorophorum*, a new, green, bloom-forming dinoflagellate (Gymnodiniales, Dinophyceae) with a vestigial prasinophyte endosymbiont. Phycologia **35**: 381—393

Felsenstein J (1993) PHYLIP (Phylogeny Inference Package) Seattle: University of Washington

Greuet C (1972) La nature trichocystaire du cnidoplaste dans le complexe cnidoplaste-nématocyste de *Polykrikos schwartzi* Bütschli. C R Acad Sci Paris **275**: 1239—1242

Greuet C (1987) Complex Organelles. In Taylor FJR (ed) The Biology of Dinoflagellates. Botanical Monographs, Vol. 21. Blackwell, Oxford, pp 119—142

Greuet C, Hovasse R (1977) A propos de la genèse des nematocysts de *Polykrikos schwartzi* Bütschli. Protistologica **13**: 145—149

Hansen G (1993) Light and electron microscopical observations of the dinoflagellate *Actiniscus pentasterias* (Dinophyceae). J Phycol **29**: 486—499

Hansen G, Daugbjerg N (2004) Ultrastructure of *Gyrodinium spirale*, the type species of *Gyrodinium* (Dinophyceae), including a phylogeny of *G. dominans*, *G. rubrum* and *G. spirale* deduced from partial LSU rDNA sequences. Protist **155**: 271—294

Hansen G, Moestrup Ø (2005) Flagellar apparatus and nuclear chambers of the green dinoflagellate *Gymnodinium chlorophorum*. Phycol Res **53**: 169—181

Hansen G, Moestrup Ø, Roberts KR (2000) Light and electron microscopical observations on the type species of *Gymnodinium*, *G fuscum* (Dinophyceae). Phycologia **39**: 365—376

Herdman EC (1921) Notes on dinoflagellates and other organisms causing discolouration of the sand at Port Erin. Proc Trans Liverpool Biol Soc **35**: 59—63

Herdman EC (1922) Notes on dinoflagellates and other organisms causing discolouration of the sand at Port Erin. II. Proc Trans Liverpool Biol Soc **36**: 15—30

Herdman EC (1923) Notes on dinoflagellates and other organisms causing discolouration of the sand at Port Erin III. Proc Trans Liverpool Biol Soc **37**: 58—63

Hoppenrath M (2000) Taxonomische und ökologische Untersuchungen von Flagellaten mariner Sande. Dissertation, University of Hamburg, 311pp

Hoppenrath M, Leander BS (2007) Character evolution in polykrikoid dinoflagellates. J Phycol **43**: In press

Horiguchi T, Pienaar RN (1991) Ultrastructure of a marine dinoflagellate, *Peridinium quinquecorne* Abé (Peridiniales) from South Africa with particular reference to its chrysophyte endosymbiont. Bot Mar **34**: 123—131

Horiguchi T, Pienaar RN (1994) Ultrastructure of a new marine sand-dwelling dinoflagellate *Gymnodinium quadrilobatum* sp. nov. (Dinophyceae) with special reference to its endosymbiotic algae. Eur J Phycol **29**: 237—245

Huelsenbeck JP, Ronquist F (2001) MrBayes: Bayesian inference of phylogenetic trees. Bioinformatics **17**: 754—755

Hulburt EM (1957) The taxonomy of unarmored Dinophyceae of shallow embayments on Cape Cod, Massachusetts. Biol Bull **112**: 196—219

Koike K, Sekiguchi H, Kobiyama A, Takishita K, Kawachi M, Koike K, Ogata T (2005) A novel type of kleptoplastidy in *Dinophysis* (Dinophyceae): presence of haptophyte-type plastid in *Dinophysis mitra*. Protist **156**: 225—237

Leander BS, Clopton RE, Keeling PJ (2003) Phylogeny of gregarines (Apicomplexa) as inferred from small subunit rDNA and beta-tubulin. Int J Syst Evol Microbiol **53**: 345—354

Lebour MV (1925) The Dinoflagellates of Northern Seas. Marine Biological Association, Plymouth, UK, 320pp

Lecal J (1972) Structure fine des Polykrikidae Kofoid et Swezy (famille de dinoflagellés). A) Étude de quelques organites de *Polykrikos grassei* nov. sp. Bull Soc Hist Nat Toulouse **108**: 302—324

Maddison DR, Maddison WP (2000) MacClade Sunderland, MA: Sinauer Associates, Inc

Matsuoka K, Fukuyo Y (1986) Cyst and motile morphology of a colonial dinoflagellate *Pheopolykrikos hartmannii* (Zimmermann) comb. nov. J Plankton Res **8**: 811—818

Nagai S, Matsuyama Y, Takayama H, Kotani Y (2002) Morphology of *Polykrikos kofoidii* and *P. schwartzii* (Dinophyceae, Polykrikaceae) cysts obtained in culture. Phycologia **41**: 319—327

Posada D, Crandall KA (1998) MODELTEST: testing the model of DNA substitution. Bioinformatics **14**: 817—818

Paulmier G (1992) Catalogue illustré des microphytes planctoniques et benthiques des côtes Normandes. Rapports internes de la Direction des Ressources Vivantes de l'IFREMER, 108pp

Saldarriaga JF, Taylor FJR, Keeling PJ, Cavalier-Smith T (2001) Dinoflagellate nuclear SSU rRNA phylogeny suggests multiple plastid losses and replacements. J Mol Evol **53**: 204—213

Saldarriaga JF, Taylor FJR, Cavalier-Smith T, Menden-Deuer S, Keeling PJ (2004) Molecular data and the evolutionary history of dinoflagellates. Europ J Protistol **40**: 85—111

Schiller J (1933) Dinoflagellatae (Peridineae) in monographischer Behandlung. In Rabenhorst's Kryptogamen-Flora von Deutschland, Österreich und der Schweiz. Band 10, Flagellatae, Abteilung 3 Dinoflagellatae (Peridineae), Teil 1. Akademische Verlagsgesellschaft, Leipzig, Germany, 617 pp

Schnepf E, Elbrächter M (1988) Cryptophycean-like double membrane-bound chloroplast in the dinoflagellate, *Dinophysis* Ehrenb: evolutionary, phylogenetic and toxicological implications. Bot Acta **101**: 196—203

Schnepf E, Elbrächter M (1999) Dinophyte plastids and phylogeny: a review. Grana **38**: 81—97

Schweikert M, Elbrächter M (2004) First ultrastructural investigations of the consortium between a phototrophic eukaryotic endocytobiont and *Podolampas bipes* (Dinophyceae). Phycologia **43**: 614—623

Shalchian-Tabrizi K, Minge MA, Cavalier-Smith T, Nedreklepp JM, Klaveness D, Jakobsen KS (2006) Combined heat shock protein 90 and ribosomal RNA sequence phylogeny supports multiple replacements of dinoflagellate plastids. J Eukaryot Microbiol **53**: 217—224

Sournia A (1986) Atlas du phytoplancton marin. Vol. 1. Éditions du Centre National de la Recherche Scientifique, Paris, 219pp

Strimmer K, Von Haeseler A (1996) Quartet Puzzling: A quartet maximum likelihood method for reconstructing tree topologies. Mol Biol Evol **13**: 964—969

Swofford DL (1999) Phylogenetic Analysis using Parsimony (and other Methods) PAUP* 40 Sunderland, MA: Sinauer Associates Inc

Tamura M, Shimada S, Horiguchi T (2005) *Galeidinium rugatum* gen. et sp. nov. (Dinophyceae), a new coccoid dinoflagellate with a diatom endosymbiont. J Phycol **41**: 658—671

Taylor FJR (2004) Illumination or confusion? Dinoflagellate molecular phylogenetic data viewed from a primarily morphological standpoint. Phycol Res **52**: 308—324

Tomas RN, Cox ER (1973) Observations on the symbiosis of *Peridinium balticum* and its intracellular alga. I. Ultrastructure. J Phycol **9**: 304—323

Uhlig G (1964) Eine einfache Methode zur Extraktion der vagilen, mesopsammalen Mikrofauna. Helgol Wiss Meeresunters **11**: 178—185

Watanabe MM, Sasa T, Suda S, Inouye I, Takichi S (1991) Major carotenoid composition of an endosymbiont in a green dinoflagellate, *Lepidodinium viride*. J Phycol **27**: 75

Westfall JA, Bradbury PC, Townsend JW (1983) Ultrastructure of the dinoflagellate *Polykrikos*. J Cell Sci **63**: 245—261

Zimmermann W (1930) Neue und wenig bekannte Kleinalgen von Neapel. Zeitschrift f Bot **23**: 419—442